Terahertz Time-Domain Spectroscopy Study of Silica Aerogels and Adsorbed Molecular Vapors

Jiangquan Zhang and D. Grischkowsky*

School of Electrical and Computer Engineering, Oklahoma State University, Stillwater, Oklahoma 74078

Received: July 14, 2004; In Final Form: September 21, 2004

We report the terahertz time-domain spectroscopy (THz-TDS) study of hydrophobic and hydrophilic silica aerogels, and the adsorption of several molecular vapors in the hydrophilic silica aerogel. The hydrophobic and hydrophilic samples have similar but discernible indices of refraction in the frequency range of 0.2−3.0 THz. Below 1.0 THz, the two samples have the same absorption, but starting from 1.0 THz, the absorption of the hydrophilic sample increases more rapidly with frequency. For the hydrophilic aerogel, a strong effect on adsorption is observed by THz-TDS for the vapors of water, heavy water, ammonia, methyl chloride, and methyl fluoride. The surface −OH groups can be replaced by −OD groups by dosing with heavy water, causing the change in the index of refraction and absorption. This replacement can be reversed by dosing the hydrophilic aerogel with water vapor. The volumetric method is used to determine the adsorption amount, which shows that the adsorbed molecules are in the submonolayer form. The equivalent index of refraction and equivalent power absorption coefficient are determined for adsorbed water, ammonia, methyl chloride, and methyl fluoride; for water and ammonia, they are quite different from the corresponding bulk properties. Dosing with hydrogen and carbon monoxide shows no observable adsorption effect.

I. Introduction

Silica aerogels[1] have attracted considerable research effort due to their unique thermal, optical, acoustical, chemical, and mechanical properties and their consequent applications in diverse areas ranging from fundamental research to the aerospace industry. Silica aerogels are composed of grains of amorphous silica with a volume porosity (air) as high as 99%, and consequently, they can be tailored to have mixed properties from both air and solid silica. These materials have been widely used in Cherenkov instrumentation for particles in a momentum range not suitable for either gas or solid radiators,[2] as they can be fabricated with a refractive index adjustable in the wide range of 1.01−1.1. Due to their very low thermal conductivity (as low as 0.003 W m^{-1} K^{-1}), aerogels are very good materials for thermal insulation.[3] Together with their high transparency property in the visible region, silica aerogels have also found applications as transparent thermal insulation in solar architecture.[4] With combinational properties of low density, fine mesostructure, and transparency, silica aerogels are also used in aerospace research for cosmic dust capture.[5]

Extensive research effort has been focused on the surface structure, surface chemistry, and adsorption processes of silica aerogels. Infrared spectroscopy has been the primary tool for these studies, as almost all the fundamental vibration frequencies of the internal bonds in silica aerogel fall in this frequency band.[6] With their enormously high internal surface areas, silica aerogels are ideal adsorbent materials for the study of adsorbed molecules and for the investigation of surface reactions. Using infrared spectroscopy, researchers have studied surface reaction and adsorption of chemical vapor molecules including H_2O, D_2O, NH_3, CH_3Cl, CH_3F, H_2, D_2, HCl, CO, etc.[6,7]

Here we report a terahertz time-domain spectroscopy (THz-TDS) study of hydrophilic and hydrophobic silica aerogels, and the adsorption of the molecular vapors of water, heavy water, ammonia, methyl chloride, and methyl fluoride in hydrophilic silica aerogel. THz-TDS has been widely used in material characterization,[8] in that THz-TDS gives information not available with other techniques in the THz (far-infrared) frequency range. Our THz-TDS study shows that the dry hydrophilic and hydrophobic silica aerogels have a similar index of refraction in the THz range, but starting from ∼1 THz, the absorption of dry hydrophilic silica aerogel increases more rapidly with frequency compared with that of the hydrophobic sample, showing that the hydrophilic Si−OH groups play an important role in the absorption above ∼1 THz.[9] The adsorption study of H_2O, D_2O, NH_3, CH_3Cl, and CH_3F in hydrophilic silica aerogel supports the above conclusion, for which it was observed that, as the hydrophilic Si−OH groups were passivated or replaced by the above adsorbed molecules, the measured absorption was reduced in the frequency range above ∼1 THz.

Dosing with H_2 and CO vapors into the hydrophilic sample chamber showed no significant effect on the dielectric properties of the sample, as no change in either the index of refraction or absorption was observed after dosing with the above vapors, indicating that the Si−OH groups are more likely to bond with strongly polarized molecules.

II. Experiment

Previously we have reported a preliminary THz-TDS study of water vapor adsorption in hydrophilic silica aerogel, where the adsorbed water showed similar properties of the index of refraction with bulk water, but different absorption properties.[10] In that study, the gravimetric method was used to measure the adsorption amount, which required a high-precision balance to be located within the vacuum system. This was a difficult

* To whom correspondence should be addressed. Phone: (405) 744-6622. Fax: (405) 744-9198. E-mail: grischd@ceat.okstate.edu.

10.1021/jp046869b CCC: $27.50 © 2004 American Chemical Society
Published on Web 11/09/2004

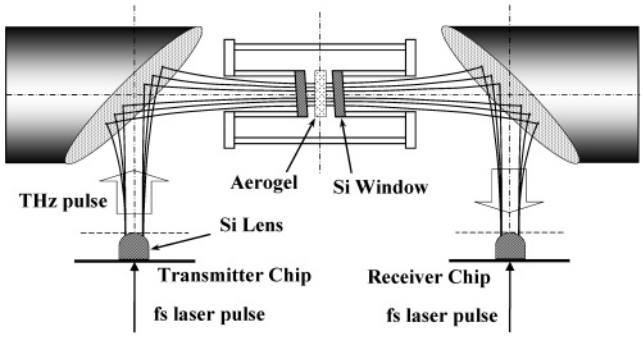

Figure 1. Experimental setup.

requirement, and the zero drift of the battery-powered balance used in the experiment[10] compromised the accuracy of the measurement. In this study, the volumetric method[11] is used to measure the adsorption amount. This method has comparatively much better accuracy and has significantly improved our results. In addition, we have been able to double the frequency range of our measurements, which now extends from 0.2 to 3 THz.

Optoelectronic generation of THz electromagnetic radiation is a newly developed source producing subpicosecond THz pulses with a wide-frequency bandwidth located midway between microwave and infrared bands. The associated THz technology has become a bridge to connect microwave technology at the low-frequency end and optical technology at the high-frequency end. A typical THz-TDS system based on this technology consists of a THz transmitter, beam collecting and steering optics, and a THz receiver. Figure 1 shows the broadband THz-TDS system[8] used in our experiment, along with the vacuum chamber containing the aerogel sample.[10] In our system, the transmitter is a photoconducting dipole antenna fabricated on a GaAs chip. This antenna is dc biased at 45 V, and when it is excited by 40 fs optical pulses with a central wavelength of 800 nm and a repetition rate of 100 MHz from a Ti:sapphire laser, THz pulses are generated with a bandwidth of 0.2−4.0 THz. A hyperspherical silicon lens is attached to the backside of the transmitter chip to collect and collimate the emitted THz pulse. The collected THz pulse has a frequency-independent beam waist located at the focal position of a paraboloidal mirror. This configuration is identical (but reversed) on the receiver side, only with the photoconducting receiver antenna fabricated on a silicon-on-sapphire chip. The incoming THz pulse induces a voltage across the unbiased receiver antenna. The receiver chip is gated by the sampling laser pulse split off from the same laser beam as the excitation laser pulse for the transmitter; a photocurrent proportional to the electrical field of the THz pulse is then generated and preamplified by a low-noise current amplifier. With the combinational use of an optical chopper and a lock-in amplifier, the amplified current can then be detected and recorded with high signal-to-noise ratio. By changing the time delay between the excitation and detection laser beams, one can obtain a THz time-domain pulse scan with both the amplitude and phase information.

The sample vacuum chamber is placed between the paraboloidal mirrors, with two high-resistivity silicon windows for the THz beam to pass through. In a standard THz-TDS system, the two identical paraboloidal mirrors are located in their confocal position. However, in our case, their separation has been extended to fit the relatively long sample vacuum chamber of 233 mm (length) × 80 mm (diameter). In the experiment, the aerogel sample is centered perpendicular to the THz beam in the center of the vacuum chamber, and can be moved in and out of the THz beam under vacuum. The two 50 mm (diameter) × 10 mm (thickness) silicon windows are tilted 3.5° relative to the aerogel sample so that the reflected THz pulses do not appear in the data scans. The window separation is minimized to 30 mm to reduce the molecular vapor absorption peaks in the spectrum. This separation is much less than the 188 mm separation used in the previous work and has enabled a significant improvement in the signal-to-noise ratio. The vacuum chamber is connected with gas sources, including H_2O, D_2O, NH_3, N_2, H_2, CO, and CH_3Cl, and each vapor can be individually dosed into the chamber.

The hydrophilic and hydrophobic silica aerogel samples used in our experiment are specified by the supplier (MarkeTech International[12]) to have an enormous surface area per mass of 800 m^2/g, corresponding to a total surface area of 2120 m^2 given the sample mass of 2.65 g for both the samples. With dimensions of 49.3 mm × 49.2 mm × 11.9 mm, the hydrophilic sample has a mass density of 0.092 g/cm^3. For the hydrophobic sample, the dimensions are 49.7 mm × 49.7 mm × 12.0 mm, resulting in a mass density of 0.089 g/cm^3. Compared with the density of 2.20 g/cm^3 for fused silica,[13] the samples contain approximately 96% free space. These materials have a typical mean pore diameter of ∼20 nm and a primary particle diameter of 2−5 nm, which is much shorter than the wavelength of the visible light. With the index of refraction very close to 1, these transparent materials have a red appearance when looked through and a blue appearance when light is reflected off the sample.

In the experiment, the volumetric method[11] was used to measure the gas adsorption in the hydrophilic silica aerogel. For this method, the sample chamber with volume V_s is valve connected to a separate dosing chamber with volume V_d, which in turn is valve connected to a cubic reference chamber with dimensions 30.5 × 30.5 × 31.0 cm^3 and volume $V_R = 28{,}840$ cm^3. To measure the volume of the dosing chamber, nitrogen gas of known pressure P_R was introduced into the reference chamber with the valved off dosing chamber under vacuum. Then the reference chamber was connected to the dosing chamber, and the equilibrium pressure P_e of the connected system was measured. The ratio of the two volumes V_d/V_R was obtained using the ideal gas law $PV = NkT$, where N is the number of gas molecules, $k = 1.38 \times 10^{-23}$ J/K is Boltzmann's constant, and $T = 295$ K is the room temperature. This ratio is given by the simple relationship $V_d/V_R = (P_R - P_e)/P_e$, which was measured to be $V_d/V_R = 0.4718$ for our system. We then reversed the procedure by pressurizing the dosing chamber with nitrogen to P_d with the reference chamber under vacuum. After the two chambers were connected, the equilibrium pressure was obtained. For this case the ratio V_d/V_R is given by $V_d/V_R = P_e/(P_d - P_e)$, which was measured to be $V_d/V_R = 0.4741$. Because of the self-consistency of these results, we believe that our pressure measurements made by MKS Baratron type 122A gauges have an accuracy of better than ±0.1 Torr. Using $V_d/V_R = 0.473 \pm 0.004$, we obtain $V_d = 13600$ cm^3 with ±1% accuracy.

The same technique was used to determine the volume V_s of the sample chamber. First the dosing chamber was pressurized to P_d with the sample chamber under vacuum. Then the two chambers were connected, and the equilibrium pressure was obtained. Following the above procedure, the ratio $V_s/V_d = 0.3129$ was measured. Using the reversed procedure, the sample chamber was pressurized to P_s with the dosing chamber under vacuum. Then the two chambers were connected, and the equilibrium pressure was obtained. For this case the ratio V_s/V_d

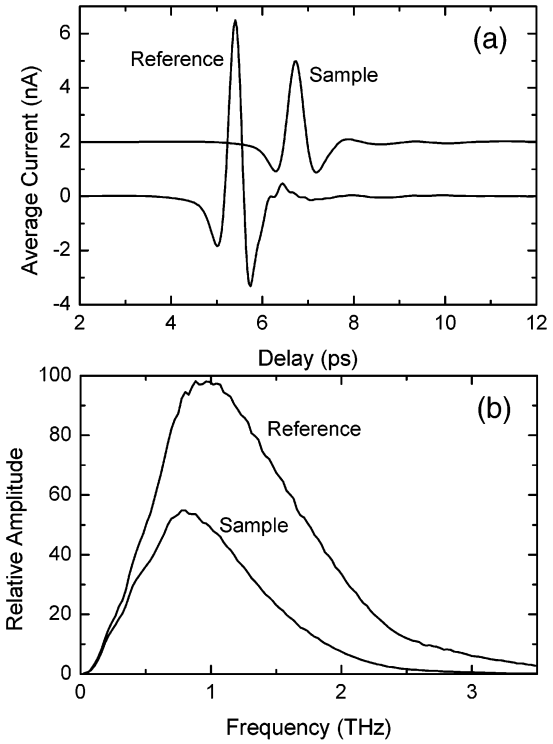

Figure 2. (a, top) Reference and sample scans for the hydrophilic silica aerogel and (b, bottom) their respective spectra. The sample pulse has been lifted up by 2 nA for clarity.

$= 0.3139$ was measured. Using $V_s/V_d = 0.314 \pm 0.003$, we obtain $V_s = 4270$ cm^3 with $\pm 1\%$ accuracy.

In the experiment, the adsorbate gas is first introduced into V_d at a known vapor pressure P_d, and then is allowed to expand into V_s. The ideal gas law is used to calculate the initial vapor pressure P_0 in the expanded system without adsorption, i.e.

$$P_0 = P_d V_d/(V_d + V_s) \tag{1}$$

When the adsorption reaches equilibrium, the equilibrium pressure P_e is measured and compared with P_0 to calculate the amount of gas adsorbed in the aerogel sample; i.e., the number of adsorbed molecules, ΔN, is calculated from

$$\Delta NkT = (P_0 - P_e)(V_d + V_s) \tag{2}$$

For eq 2 the pressures P_0 and P_e must be stated in pascals for which the conversion between pascals and torr is 1 Torr $=$ 133.32 Pa. In addition, the volumes V_d and V_s must be stated in cubic meters.

III. Results and Discussion

1. Hydrophilic vs Hydrophobic Silica Aerogel. For the hydrophilic silica aerogel, the hydrophilicity is mainly caused by the Si−OH groups.[9,14] The terminal hydroxyl groups promote the adsorption of water and other polar molecules, and the amount of water adsorption is directly related to the number of surface hydroxyl groups.[15] On the other hand, hydrophobicity is achieved by replacing the hydroxyl groups by hydrolytically stable nonpolar chemical groups, such as Si−CH_3.[15,16] This procedure can be done by hydrolysis in methyltrimethoxysilane (MTMS) and tetramethoxysilane (TMOS) followed by supercritical drying in methanol.[9,14] By heating the hydrophobic aerogel in air at above 200 °C, the −CH_3 groups react with O_2 and transform to −OH groups, resulting in hydrophilicity in the aerogel.[9]

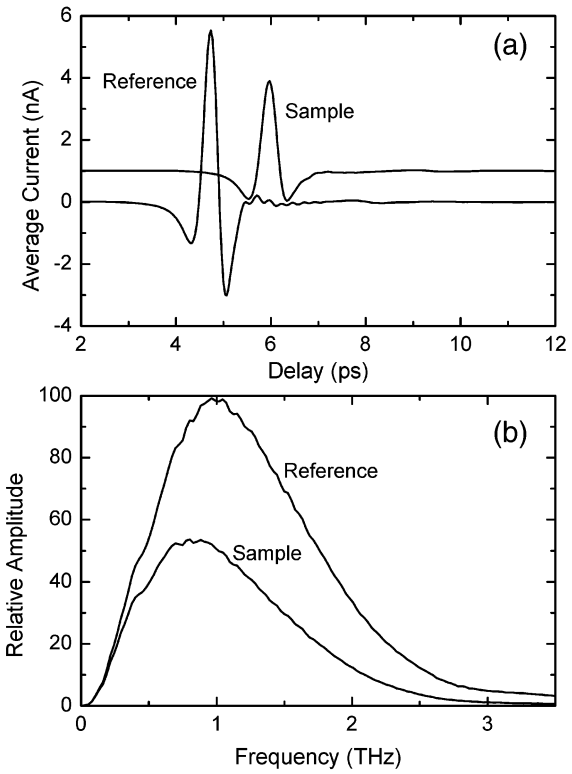

Figure 3. (a, top) Reference and sample scans for the hydrophobic silica aerogel and (b, bottom) their respective spectra. The sample pulse has been lifted up by 1 nA for clarity.

As the initial investigation, we compare the difference between the dry hydrophilic and hydrophobic silica aerogels in terms of the index of refraction and the power absorption coefficient. Up to now, the extensive spectroscopy research effort on aerogels has been focused in the optical and infrared region, while study in the far-infrared (THz) has been neglected. In this experiment, the reference THz pulse was obtained by moving the aerogel sample out of the THz beam, while the sample pulse was measured with the sample in the beam; both pulses were obtained under vacuum. Figure 2a shows the output pulses of the reference and sample scans for the hydrophilic silica aerogel sample, along with their respective spectra in Figure 2b. The corresponding results for the hydrophobic sample are shown in Figure 3. The time delays and amplitude reductions of the sample pulses were caused by the aerogel samples. Due to the frequency-dependent power absorption coefficient, the sample pulse shapes and widths also changed slightly, compared with those of the reference pulse.

The indices of refraction and the power absorption coefficients for both the hydrophilic and hydrophobic silica aerogels are presented in Figure 4. The indices of refraction of the two samples show discernible differences within the frequency range of the spectrometer. It is known that the index of refraction of the aerogel is scalable to its density, and that the relation between the index of refraction and the density can be written as $n = 1 + K\rho$.[17,18] With $\rho_{SiO_2} = 2.20$ g/cm^3 and $n_{SiO_2} = 1.96$ in the THz range for fused silica,[8] the coefficient of proportionality is determined as $K = (n_{SiO_2} - 1)/\rho_{SiO_2} = 0.436$ cm^3/g. From Figure 4a, at 1.0 THz, the indices of refraction are 1.0341 for the hydrophilic sample and 1.0317 for the hydrophobic one. Along with the mass densities for the two samples, the measured results are $K = 0.371$ cm^3/g for the hydrophilic sample and $K = 0.355$ cm^3/g for the hydrophobic one, which are, respectively, 15% and 19% lower than that determined from fused silica. This observation is consistent with the results in the optical frequency

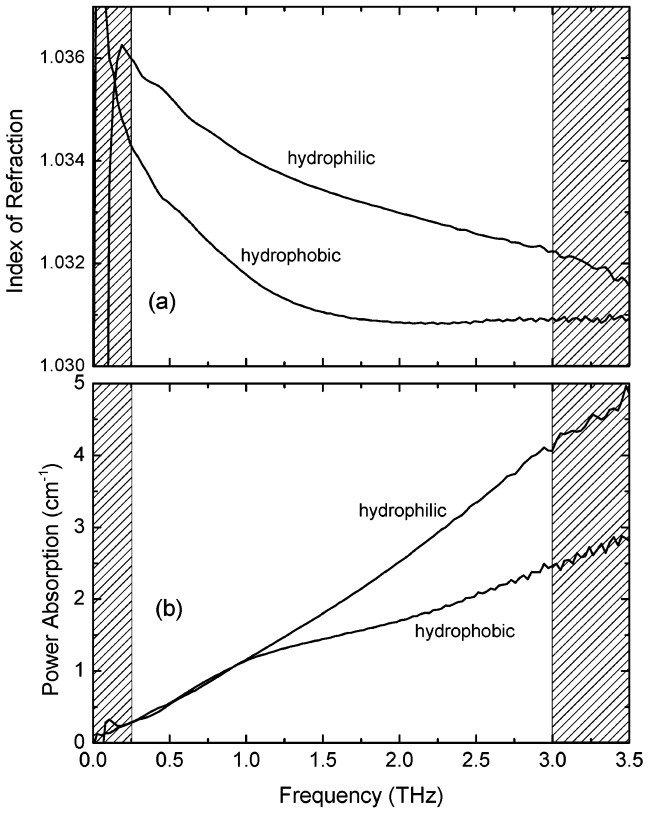

Figure 4. (a) Indices of refraction and (b) power absorption coefficients of hydrophilic and hydrophobic silica aerogels. Measurements are not considered accurate in the shaded regions.

range, where for light aerogel ($\rho \leq 0.1$ g/cm^3) the measured K is also smaller than that determined from fused silica.[18]

It is also noteworthy that, for fused silica, the index of refraction increases monotonically with frequency in the THz range,[8] while for the aerogel, it decreases with frequency. This result is clearly inconsistent with the assumed scalability of the index of refraction, and further investigation is needed for this property.

Although the index of refraction is scaled down in aerogel according to its density, the absorption is comparatively much higher and is comparable with that of fused silica. From Figure 4b, at 2.0 THz, the power absorption coefficient is 2.5 cm^{-1} for the hydrophilic silica aerogel, compared with 8.0 cm^{-1} for fused silica.[8] At frequencies between 0.2 to 1.0 THz, the power absorption coefficients of dry hydrophilic and hydrophobic aerogels are essentially the same. However, at above 1.0 THz, the absorption of hydrophilic aerogel increases more rapidly with frequency. We consider that the Si−OH groups in the hydrophilic sample are responsible for the absorption increase above 1.0 THz. This will be later shown to be consistent with the observations of the water adsorption experiment.[10]

2. Treatment of Hydrophilic Silica Aerogel with Water and Heavy Water Dosing. Heavy water (D_2O) has been used to study the spectroscopy structure of the terminal Si−OH groups in the hydrophilic silica aerogel in that the −OH groups can be easily replaced by the isotropic −OD groups by exposing the sample to D_2O vapor.[6,7] Infrared spectroscopy has been used to confirm this replacement, as the characteristic stretching frequency of −OH groups around 3750 cm^{-1} moved to a lower frequency of ∼2760 cm^{-1}, which is the stretching frequency of −OD groups.[7] It is found that this replacement is totally reversible by exposing the sample to saturated water vapor.[19] The replacement of −OH groups by −OD groups and the reverse replacement can both be done at room temperature, making this an appropriate technique to study the terminal −OH groups.

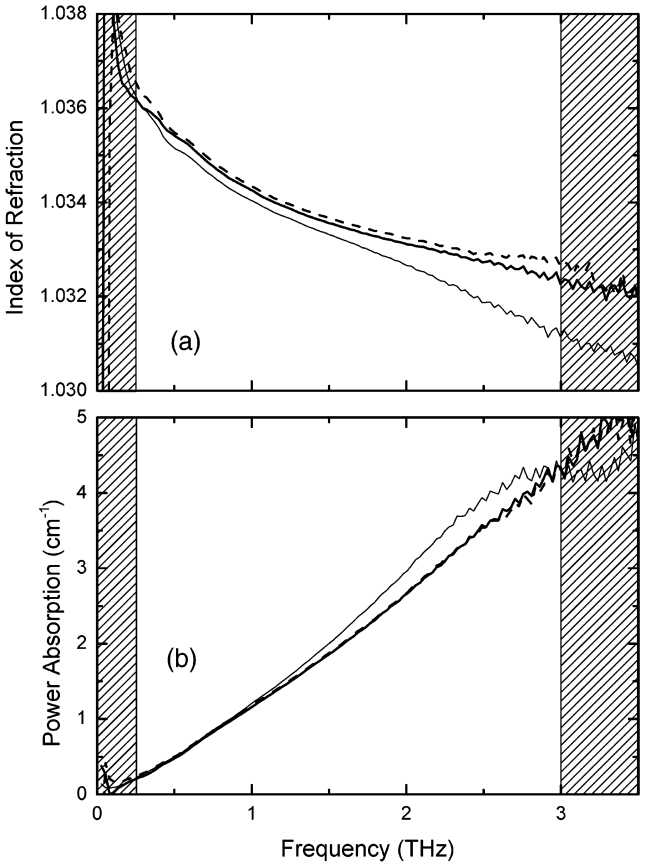

Figure 5. (a) Index of refraction and (b) power absorption coefficient of hydrophilic silica aerogel: thick solid line, before D_2O dosing; thin solid line, after D_2O dosing; thick dashed line, after H_2O dosing.

Here we examine by THz-TDS the treatment of hydrophilic silica aerogel with heavy water (D_2O) and water (H_2O) vapor dosing. The sample chamber containing the hydrophilic silica aerogel was first pumped down to below 50 mTorr to allow full desorption for the sample. For future comparison, a reference pulse without the sample in the THz beam and a signal pulse with the sample in the THz beam were measured to obtain the initial index of refraction and power absorption coefficient. The aerogel sample was then treated with heavy water (D_2O) vapor in the following procedure. First, the sample chamber was dosed with D_2O vapor and kept at 10 Torr for about 1 h for the adsorption to equilibrate, and then the chamber was pumped down to below 100 mTorr. The chamber was dosed again with D_2O vapor at 10.0 Torr for 5 min and pumped down. This process was repeated three times, and the −OH groups on the surfaces of silica aerogel were considered to be completely replaced by −OD groups. Another set of THz reference and signal scans were measured to obtain the dielectric properties of aerogel with −OD groups. After this, the aerogel sample was treated with normal water (H_2O) vapor, in the same way as the above D_2O treatment, to restore the −OH groups from −OD groups on the silica aerogel surfaces. Again we took the THz reference and signal scans after the sample chamber was pumped down for a complete desorption of water molecules from the aerogel sample.

Figure 5 presents the refractive index and power absorption coefficient of the dry hydrophilic silica aerogel before the D_2O treatment, after the D_2O treatment, and after the following H_2O

treatment. It is shown in Figure 5a that, after the D_2O treatment, the refractive index decreased, indicating that the index of refraction is substantially affected by the terminal groups on the silica surface. In Figure 5b, the power absorption coefficient is essentially the same below ~1 THz for the sample before and after the D_2O treatment, but starting from 1 THz, the measured absorption is higher for the sample after D_2O treatment than that before the treatment. This observation is consistent with the result in section 1 that the −OH groups play an important role in the absorption in the frequency range above ~1 THz. Here, the replacement of −OH groups with −OD groups caused the absorption increase in the frequency range above ~1 THz.

It is also noteworthy that, after the following water treatment, both the refractive index and power absorption coefficient were almost restored to their original values, indicating that the −OH and −OD groups are fully convertible. This is consistent with the conclusion of the previous investigation in the infrared range that the replacement of −OH with −OD is fully reversible.[19]

3. Water Adsorption. Now we study the water adsorption in hydrophilic silica aerogel by THz-TDS. It is well-known that the Si−OH groups are responsible for the hydrophilicity. We have shown in section 1 that the hydroxyl groups caused the absorption increase in the frequency range above ~1 THz. When water vapor is dosed in the sample, as the hydroxyl groups are bonded with water molecules, an absorption change is expected. In addition, the adsorbed water molecules will cause an increase in absorption, so the overall results will be a combination of the two effects.

For this experiment, the sample chamber was first pumped down to below 50 mTorr to allow a complete desorption for the hydrophilic silica aerogel. A reference scan was then taken with the dry aerogel sample in the THz beam. Initially, the dosing chamber was filled with 1.50 Torr of water vapor, and then the sample chamber was opened to the water vapor; the water adsorption occurred immediately. Without adsorption, the initial pressure in the connected system can be calculated from eq 1 to be $P_0 = 1.14$ Torr. After about 20 min, the connected system reached an equilibrium vapor pressure of 0.54 Torr; the pressure drop compared to P_0 was due to the water adsorption in the aerogel sample. A sample scan was taken at this equilibrium pressure.

To increase the water adsorption and the equilibrium pressure, the sample chamber was valved off from the dosing chamber; the dosing chamber was then filled with a higher pressure of water vapor. After the water source was closed, the sample chamber was again connected to the dosing chamber to allow the water vapor to reach adsorption equilibrium with the aerogel sample, which takes approximately 20 min. Another sample scan was taken at this new equilibrium pressure. This procedure was repeated several times, each time with increased water dosing pressure, and hence increased water adsorption and equilibrium vapor pressure. As a result, we have measured the sample scans at a series of equilibrium vapor pressures of 0.54, 0.97, 1.48, 2.22, 3.11, 4.70, 6.31, 8.36, and 13.59 Torr.

Figure 6a shows the output pulse at the adsorption equilibrium water vapor pressure of 0.97 Torr; the output pulses at the other equilibrium pressures are similar. The inset of Figure 6a is the enlargement of the reference scan under vacuum and the sample scans at the equilibrium vapor pressures of 0.97, 4.70, 8.36, and 13.59 Torr at the vicinity of the main peaks, which shows the increased delay and intensity drop of the THz pulses caused by the increased water adsorption.[10]

The corresponding spectra of the output pulses of the inset of Figure 6a are shown in Figure 6b; the sharp spikes in the

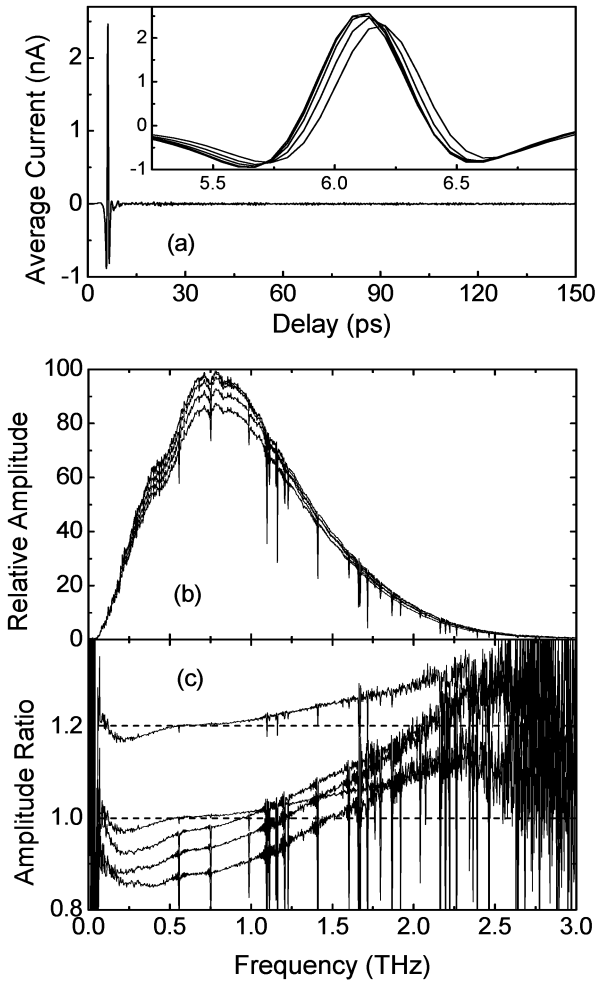

Figure 6. (a) Output pulse at the adsorption equilibrium water vapor pressure of 0.97 Torr. The inset is the reference scan under vacuum and the sample scans at the equilibrium vapor pressures of 0.97, 4.70, 8.36, and 13.59 Torr (from left to right) at the vicinity of the main peaks; their respective spectra are shown in (b). (c) Amplitude spectrum ratios between scans at different vapor pressures (from top to bottom, 0.97, 4.70, 8.36, and 13.59 Torr) and that under vacuum. The top curve is the spectrum ratio between the 0.97 Torr and vacuum scans shifted up by 0.2 for clarity.

spectra are the absorption lines from water vapor. To more clearly present the spectral amplitude changes of the scans under different vapor pressures, we show in Figure 6c the corresponding spectral amplitude ratios between the scans at different water vapor pressures and that under vacuum; the ratio for 0.97 Torr is repeated and shifted up by 0.2 for clarity. From Figure 6c, at a low dosing vapor pressure of 0.97 Torr, the amplitude decrease below 0.56 THz and the increase above 0.56 THz are clearly seen. As the dosing vapor pressure goes up to 4.70 Torr, the spectrum amplitude above 1.17 THz continues to increase, but the amplitude below 1.17 THz drops lower. As the vapor pressure continues to increase, the spectral amplitude decreases in the entire frequency range from 0.2 to 3.0 THz, causing the cross point between the spectra of the original aerogel under vacuum and the sample with adsorbed water to move to higher frequency. However, even at 13.59 Torr, the THz transmission of the sample with adsorbed water is still higher than that of the original sample at the high-frequency end.

As stated above, the overall absorption is the combinational result of the absorption change due to the −OH groups being passivated by the adsorbed water, and the increased absorption caused by the adsorbed water itself. At the higher frequency

TABLE 1: Experimental Adsorption Results of Several Molecular Vapors

	water	ammonia	methyl chloride	methyl fluoride
molecular formula	H_2O	NH_3	CH_3Cl	CH_3F
molecular mass (g)	2.99×10^{-23}	2.82×10^{-23}	8.38×10^{-23}	5.65×10^{-23}
liquid density (g/cm^3)	1.000	0.817 (−79 °C)[13]	0.920 (18 °C)[13]	0.579
molecular diameter[a] (nm)	0.31	0.33	0.45	0.46
dosing pressure P_d (Torr)	25.83	89.93	97.87	90.22
initial pressure P_0 (Torr)	19.66	68.44	74.48	68.66
equilibrium pressure P_e (Torr)	13.20	62.83	73.57	68.19
adsorbed no. of molecules ΔN	3.78×10^{21}	3.28×10^{21}	5.35×10^{20}	2.76×10^{20}
adsorbed mass (mg)	113	92.5	44.8	15.6
adsorbed volume (cm^3)	0.113	0.113	0.0487	0.0269
total layer thickness (nm)	0.053	0.053	0.023	0.013
no. of monolayers	0.17	0.16	0.05	0.03
effective thickness d_E (μm)	46.6	46.7	20.1	11.1

[a] The molecular diameters are calculated directly from the molecular mass and liquid density.

end, the initial decrease in absorption at low dosing water vapor pressure indicates that the absorption change is dominated by the absorption decrease of the passivated −OH groups. As the dosing pressure increases, as more and more −OH groups are passivated, intuitively the absorption should continue to drop. However, the observed absorption starts to increase at a certain dosing vapor pressure. This contradiction indicates that the water molecules adsorbed later are not directly bonded to the −OH groups, which only serve as absorption centers. Hence, above a certain vapor pressure, the absorption increases for all the frequencies with the vapor pressure. It has been shown that, at very low water vapor pressure, the initial adsorption starts on the surface hydroxyl sites.[20] As the vapor pressure increases, the following adsorption covers more hydroxyl sites, and at the same time water molecule clusters also build up around these sites; these water clusters are believed to be responsible for the broad-band absorption increase as the dosing pressure increases. The adsorption only occurs on the surface hydroxyl sites, while the portions of silica surfaces without hydroxyl groups are not covered with water molecules even at pressures close to saturation.[15]

At a low dosing vapor pressure (0.97 Torr), the immediate absorption increase at frequencies below 0.56 THz indicates that the absorption is overwhelmingly from the adsorbed water. In the frequency range from 0.56 to 1.17 THz, however, the initial absorption change is overwhelmed by the decreased absorption due to the passivated −OH groups, but the absorption due to the adsorbed water soon takes over the domination at relatively low dosing pressure compared with that at higher frequencies. This result clearly shows the frequency dependence of the absorption change due to adsorbed water in the hydrophilic silica aerogel.

We now look at the overall effect in terms of equivalent refractive index and equivalent power absorption coefficient.[10] A separate experiment was conducted for this purpose, for which the dosing chamber was used to dose the sample chamber, as described in the Experiment. The dosing procedure was as follows. Both the dosing and sample chambers were first pumped down to below 50 mTorr. The dosing chamber was filled with 18.04 Torr of water vapor, then the water source was closed off, and the sample chamber was opened to the water vapor; the water adsorption immediately occurred in the aerogel sample. After about 8 min, the vapor pressure in the connected dosing chamber−sample chamber system dropped to 10.24 Torr due to the adsorption; the sample chamber was then closed from the dosing chamber. The dosing chamber was then refilled with water vapor to 18.03 Torr, and then closed from the water source. The sample chamber (with vapor pressure originally at 10.24 Torr but continuously dropping due to adsorption) was reconnected with the dosing chamber. In this experiment, the equivalent initial dosing pressure was $P_d = 18.04 + 18.03 - 10.24$ Torr $= 25.83$ Torr, and the equivalent initial vapor pressure in the expanded system without adsorption was then calculated as $P_0 = 19.66$ Torr. Given that the actual equilibrium vapor pressure with adsorption is $P_e = 13.20$ Torr, the number of adsorbed water molecules is then calculated from eq 2 to be $\Delta N = 3.78 \times 10^{21}$. Knowing that the mass of the water molecule is 2.99×10^{-23} g, this is equivalent to 113 mg in mass, or 0.113 cm^3 in bulk volume. Given the total surface area of 2120 m^2 inside the aerogel, this adsorption amount is equivalent to a surface water layer thickness of 0.053 nm, or 0.17 monolayer thickness of water, indicating that the adsorbed water is in submonolayer form. The above dosing and adsorption calculation results are listed in Table 1.

As an independent check on the mass of the adsorbed water by the aerogel, a simple mechanical balance was constructed in our laboratory. This balance had a repeatable accuracy of ±2 mg and could be operated in our cubic reference chamber, and the measurement under vacuum could be read through the large window of the chamber. The hydrophilic aerogel sample was placed in this reference chamber, and the chamber was pumped down to dry out the aerogel. Then, after continuous exposure to water vapor at 13.2 Torr, a steady-state mass gain of 114 mg of the aerogel was obtained. This value is in good agreement with our above results obtained by the more accurate volumetric method.

To characterize the adsorbed water submonolayer by THz-TDS, four measurements of different transmitted THz pulses were performed, a reference scan under vacuum without the sample, with its complex spectrum amplitude denoted by $A_0(\omega)$, a dry sample scan under vacuum before the water dosing, denoted by $A_a(\omega)$, a sample scan after the water dosing at 13.20 Torr and with 13.20 Torr in the sample chamber, denoted by $A_{a+aw+v}(\omega)$, and a reference scan without the sample but with 13.20 Torr of water vapor pressure in the chamber, denoted by $A_v(\omega)$, where ω is angular frequency. Figure 7a shows the output pulses of sample scans before and after the water dosing; the inset is the enlargement of the pulses at the vicinity of the main peaks, which shows that the signal pulse is delayed by approximately 0.09 ps relative to the reference pulse, caused by the adsorbed water.[10] The corresponding spectra and their amplitude ratio are presented in parts b and c, respectively, of Figure 7. Compared with the scanning range of 100 ps used in the previous measurement,[10] we have extended the scanning range to 153 ps, for which the spectral resolution is significantly increased. Hence, it is much easier to separate the broad

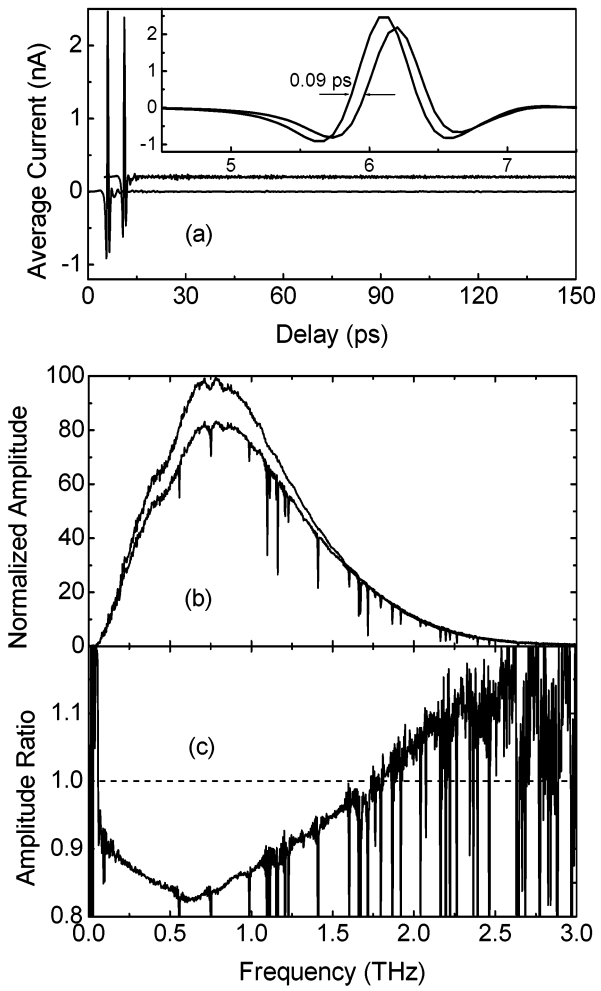

Figure 7. (a) Output pulses, (b) respective spectra of hydrophilic silica aerogel before and after 13.20 Torr water vapor dosing, and (c) amplitude ratio between the two spectra. The sample scan pulse has been shifted for clarity. The inset of (a) shows the enlargement of the output scans at the vicinity of the main peaks.

absorption of the water layer from the sharp water lines. In fact, some of the water lines previously entangled together are now well resolved.[10,21] It is also noted that the water lines appear to be weaker when compared with the previous measurement at similar pressure.[10] This is because the THz beam path of 30 mm in the water vapor (separation between the silicon windows) is much shorter than the previous path length of 188 mm.[10]

The complex amplitude spectrum of the signal pulse of the aerogel sample in a vacuum can be written as

$$A_a(\omega) = A_0(\omega)\, H_a(\omega) \tag{3}$$

while for the water vapor in the chamber without the aerogel sample in the THz beam, this relation is

$$A_v(\omega) = A_0(\omega)\, H_v(\omega) \tag{4}$$

Here, $A_0(\omega)$ is the complex spectrum of the vacuum reference pulse without the aerogel sample in the THz beam and $H(\omega)$ designates the complex frequency transfer functions for the different conditions indicated by the subscripts. We use the subscripts a, v, and aw to denote aerogel, water vapor, and adsorbed water, respectively, so $H_{a+aw}(\omega)$ is the complex frequency transfer function of the aerogel with adsorbed water, and so on. The complex spectrum of the signal pulse of the aerogel sample with adsorbed water and water vapor in the sample chamber can be written as

$$A_{a+aw+v}(\omega) = A_0(\omega)\, H_{a+aw}(\omega)\, H_v^{\,x}(\omega) \tag{5}$$

If the transfer function for the water vapor were the same with and without the aerogel sample in the THz beam, the exponential factor x in the above equation would be 1.[10] However, since the 30 mm separation between the silicon windows is comparable with the 11.9 mm thickness of the aerogel sample, we cannot assume that this function is the same for both the cases, and consequently, x has to be determined.

With these relations the effect caused by the adsorbed water in the aerogel can now be extracted as[10]

$$H_{aw}(\omega) = \frac{H_{a+aw}(\omega)}{H_a(\omega)} = \frac{A_{a+aw+v}(\omega)}{A_a(\omega)}\left[\frac{A_0(\omega)}{A_v(\omega)}\right]^x \tag{6}$$

With this equation, the exponential factor x is determined as 0.82 by minimizing the spikes caused by the water vapor in the amplitude part of $H_{aw}(\omega)$. This method of determining x is physically reasonable in that the vapor transfer function is exponentially scalable with the propagation length of the THz beam in the vapor.

In calculating an equivalent refractive index and equivalent power absorption coefficient of the adsorbed water, an equivalent sample thickness of bulk water is calculated as $d_E = 46.6$ μm by dividing the 0.113 cm^3 bulk volume of adsorbed water by the 4.928 cm $\times$ 4.924 cm cross-sectional area of the sample. The equivalent refractive index $n_{aw}^E(\omega)$ and the equivalent power absorption coefficient $\alpha_{aw}^E(\omega)$ of the equivalent water layer of thickness d_E are defined by the relationship[10]

$$H_{aw}(\omega) \equiv \exp\left\{i\frac{2\pi d_E}{\lambda_0}[n_{aw}^E(\omega) - 1]\right\} \exp[-\alpha_{aw}^E(\omega) d_E/2] \tag{7}$$

where λ_0 is the free-space wavelength. It should be understood that the definition of eq 7 is not a real measurement of the adsorbed water, in that the adsorbed water is in the submonolayer form, while this definition is for an equivalent bulk volume. In addition, the measured phase shifts responsible for determination of $n_{aw}^E(\omega)$ and the measured absorption responsible for determination of $\alpha_{aw}^E(\omega)$ include effects due to passivating the $-$OH groups. Nevertheless, we can still use this simple definition to examine the overall effect caused by the adsorbed water.

The calculated $n_{aw}^E(\omega)$ and $\alpha_{aw}^E(\omega)$ from eq 7 with $d_E = 46.6$ μm are presented in Figure 8, together with the index of refraction and the power absorption coefficient for bulk water,[10] although the measurements presented in Figure 8 appear to disagree with the earlier work[10] in the comparable frequency ranges. This apparent disagreement is explained by the fact, that in the previous report, we did not have an accurate measurement of the adsorption amount. Consequently, in that report, we adjusted the layer thickness d_E to force the obtained $n_{aw}^E(\omega)$ to match the known index of refraction of bulk water.[10] Here, if we used the same method of a forced fit, we would obtain similar results in the frequency range from 0.2 to 1.5 THz. However, we now have a good measure of $d_E = 46.6$ μm from the volumetric method. In addition, our current measurement has increased the bandwidth to 3.0 THz, 2 times that for the previous work.[10] The signal-to-noise ratio is also substantially improved, mainly due to the reduced distance between the silicon windows, thereby significantly suppressing the observed strong water vapor lines. Consequently, the $n_{aw}^E(\omega)$

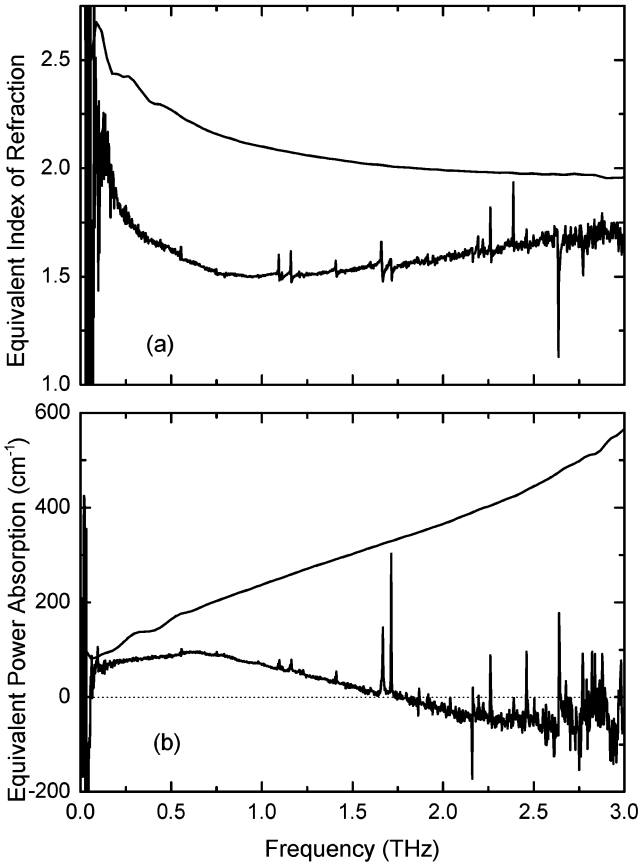

Figure 8. (a) Equivalent indices of refraction and (b) equivalent power absorption coefficients of the adsorbed submonolayer water (bottom curves) and bulk water (top curves).

and $\alpha_{aw}^{E}(\omega)$ curves are much cleaner. As stated above, the results in Figure 8 are combinational effects of the adsorbed submonolayer molecules and the passivated −OH groups; as can be seen they are quite different from those of the bulk water.[11]

From Figure 8b, at frequencies below ~0.6 THz, the measured $\alpha_{aw}^{E}(\omega)$ increases monotonically with frequency, just like that for bulk water. However, starting from the turning point of ~0.6 THz, $\alpha_{aw}^{E}(\omega)$ decreases monotonically with frequency. This result is consistent with the observation that the absorption properties at low frequencies are dominated by the adsorbed water, while at higher frequencies, the absorption is a competing effect between the adsorbed water (increased absorption) and the passivated −OH groups (decreased absorption).

4. Ammonia Adsorption. Ammonia has been extensively studied by microwave and infrared spectroscopy. With the development of THz technology, far-infrared THz-TDS studies of bulk ammonia[22] and ammonia vapor[23] have also been reported. Ammonia has also been used to study the properties and surface structures of silica aerogel.[6,7] The interaction of nitrogen lone-pair electrons with the surface hydroxyl groups in hydrophilic silica aerogel results in the ammonia adsorption, which can take place at room temperature. The ammonia adsorption can be completely removed by evacuation at room temperature.[7] It is also found that ammonia chemisorption can occur in deuterated silica aerogel, in which part of the Si−OD groups transformed into Si−NH_2 groups.[7]

Here, we investigate ammonia adsorption in hydrophilic silica aerogel by THz-TDS. Again, the volumetric method is used to calculate the adsorption volume. For this experiment, the dosing procedure is similar to that for the water adsorption, except that

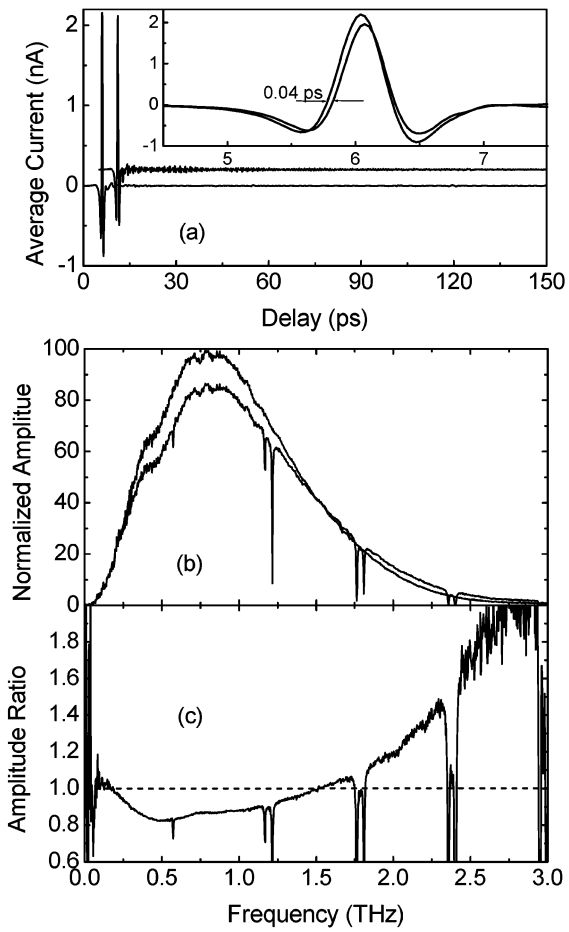

Figure 9. (a) Output pulses, (b) respective spectra of hydrophilic silica aerogel before and after the ammonia vapor dosing, and (c) amplitude ratio of the two spectra. The sample scan pulse has been shifted for clarity. The inset of (a) shows the enlargement of the output scans at the vicinity of the main peaks.

the dosing chamber was only filled once. The dosing and adsorption results are listed in Table 1, which shows that the adsorbed ammonia covers 0.17 monolayer on the silica surface. Like the adsorbed water, the adsorbed ammonia is also in submonolayer form.

As in the THz-TDS experiment with water adsorption, four scans were obtained, i.e., a reference scan under vacuum, a sample scan under vacuum, a sample scan after ammonia adsorption, and a reference scan at the same ammonia vapor pressure. The output pulses of the sample scans are presented in Figure 9a; the inset of Figure 9a is the enlargement of the output pulses at the vicinity of the main peak, which shows that the signal pulse is delayed by approximately 0.04 ps relative to the reference pulse, caused by the adsorbed ammonia. The corresponding spectra and their amplitude ratio are shown in parts b and c, respectively, of Figure 9. The sharp absorption lines in Figure 9b are caused by the ammonia vapor.[23] Similar to that observed in the water adsorption experiment, a cross point between the two frequency-domain spectra is seen. This observation shows that the adsorbed ammonia has passivating and absorption effects similar to those of the adsorbed water.

We now follow the same procedure as in the water adsorption experiment to analyze the adsorbed ammonia. Equations 3−7 are still valid for this case, with the understanding that now the subscripts v and aw stand for ammonia vapor and adsorbed ammonia, respectively. As shown in Table 1, the equivalent bulk layer thickness for the calculation of the equivalent

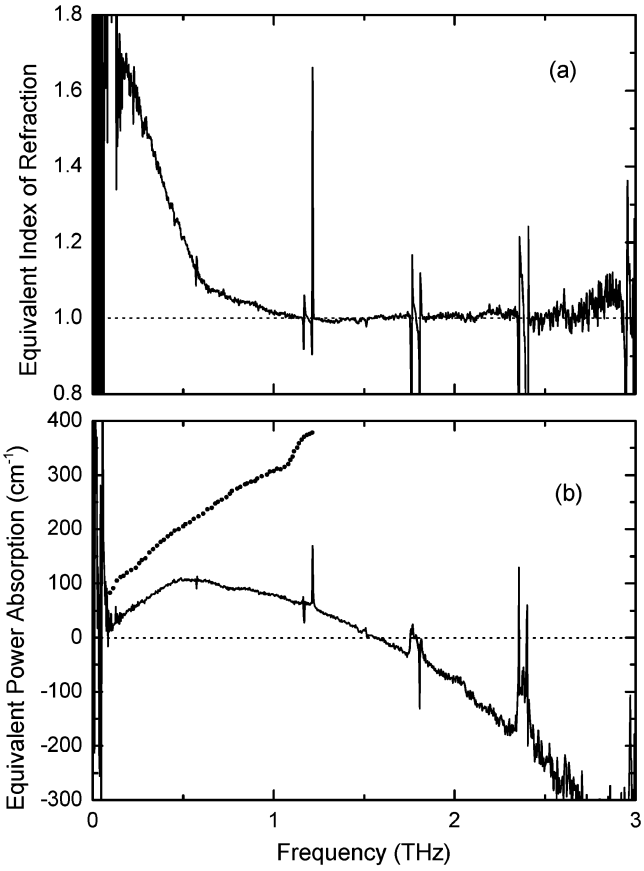

Figure 10. (a) Equivalent index of refraction and (b) equivalent power absorption coefficient of the adsorbed submonolayer ammonia. The dotted curve in (b) is the power absorption coefficient of liquid ammonia at −33 °C.[22]

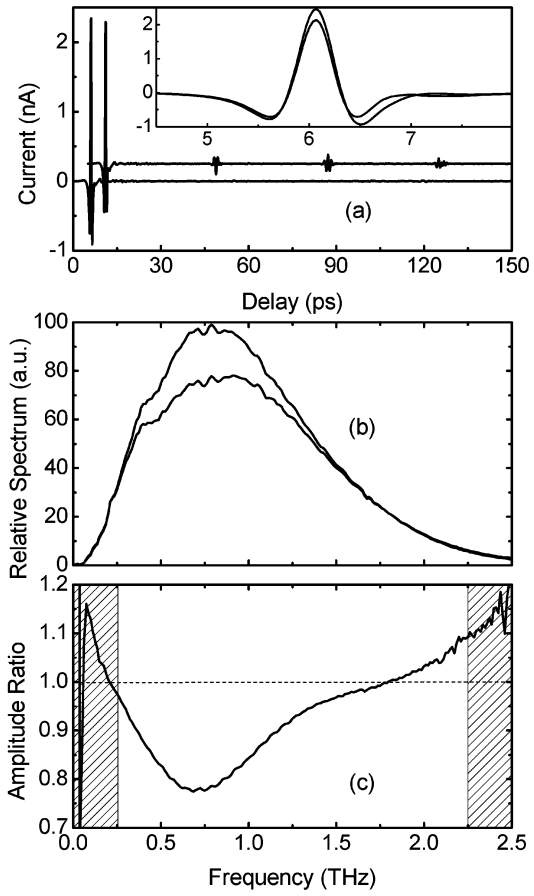

Figure 11. (a) Output pulses of hydrophilic silica aerogel before and after CH_3Cl vapor dosing. (b) Spectra of the main pulses in the time range 0−40 ps and (c) amplitude ratio between the two spectra. The sample scan pulse has been shifted for clarity. The inset of (a) shows the enlargement of the output scans at the vicinity of the main peaks.

refractive index and the equivalent power absorption coefficient was calculated as $d_E = 46.7\ \mu$m. The power transfer function of the adsorbed ammonia is calculated from eq 6, with the exponential factor determined as $x = 0.90$ by minimizing the spikes in the resulting amplitude part of $H_{aw}(\omega)$. From the resulting $H_{aw}(\omega)$, the equivalent index of refraction $n^E_{aw}(\omega)$ and the equivalent power absorption coefficient $\alpha^E_{aw}(\omega)$ of the equivalent ammonia layer are calculated from eq 7 and presented in Figure 10. Due to the difficulties in preparing the samples, the dielectric properties of liquid ammonia have rarely been reported in the far-IR range. Figure 10b also shows the previously measured power absorption coefficient of liquid ammonia at −33 °C.[22] However, the refractive index of liquid ammonia is not readily available in the THz range. The measured $n^E_{aw}(\omega)$ of the adsorbed ammonia is extremely low compared with that of adsorbed water; starting from 1.2 THz, the refractive index is almost flat near 1, while at lower frequencies it increases as frequency decreases. The measured $\alpha^E_{aw}(\omega)$ of adsorbed ammonia has a frequency dependence similar to that of $\alpha^E_{aw}(\omega)$ of adsorbed water. This is not surprising in that the measured power absorption of liquid ammonia also has a frequency dependence similar to that of the measured power absorption of bulk water.[22]

5. Adsorption with Methyl Chloride and Methyl Fluoride. THz-TDS has been previously used to study the rotational lines of methyl chloride (CH_3Cl) and methyl fluoride (CH_3F) vapors.[24,25] Unlike water vapor, CH_3Cl and CH_3F vapors are known to have rotational absorption lines separated by an almost constant frequency spacing. When THz pulses pass through the vapors, a manifold of rotational lines are excited; the molecules then reradiate a free-induction decay signal consisting of a series of uniformly spaced pulses, which have been termed THz commensurate echoes.[24−26]

Here we use THz-TDS to investigate the adsorption of CH_3Cl and CH_3F in hydrophilic silica aerogel. The experiment and calculation procedures were similar to those for the adsorption of water vapor and ammonia. The dosing and adsorption results of both CH_3Cl and CH_3F are listed in Table 1, which again shows that the adsorbed CH_3Cl and CH_3F are in submonolayer form. Compared with the results of the adsorption of water and ammonia, the numbers of adsorbed molecules for CH_3Cl and CH_3F are approximately 1 order of magnitude lower, showing a weaker adsorption of the CH_3Cl and CH_3F by the aerogel sample. Four THz scans were taken for each of the vapors, the same as those in the adsorption of water vapor and ammonia.

Figure 11a shows the THz pulses after propagation through the hydrophilic silica aerogel in a vacuum and after the CH_3Cl adsorption; the sample pulse in CH_3Cl vapor has been shifted for clarity. As observed in earlier reports,[24,25] here the sample scan is composed of the main transmitted pulse and the following equally spaced coherent transients. The inset of Figure 11a is the enlargement of the pulses in the vicinity of the main transmitted pulses. Contrary to thsoe observed in the adsorption of water vapor and ammonia, here the two pulses show no significant time delay. The respective spectra of the main transmitted pulses in the time range of 0−40 ps are presented in Figure 11b; the corresponding spectrum ratio is shown in Figure 11c. As in the adsorption of water vapor and ammonia, the adsorption of CH_3Cl exhibits similar properties. An adsorp-

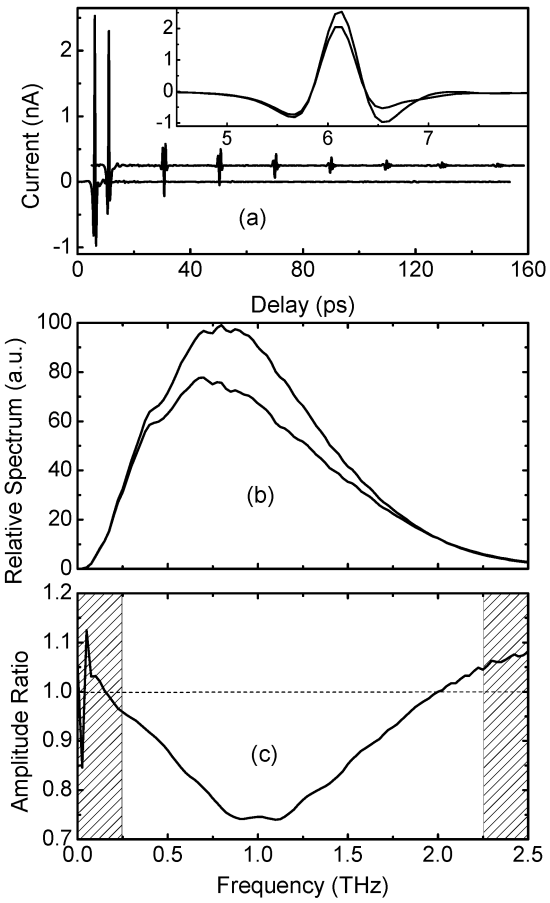

Figure 12. (a) Output pulses of hydrophilic silica aerogel before and after CH_3F vapor dosing. (b) Spectra of the main pulses in the time range 0−20 ps and (c) amplitude ratio between the two spectra. The sample scan pulse has been shifted for clarity. The inset of (a) shows the enlargement of the output scans at the vicinity of the main peaks.

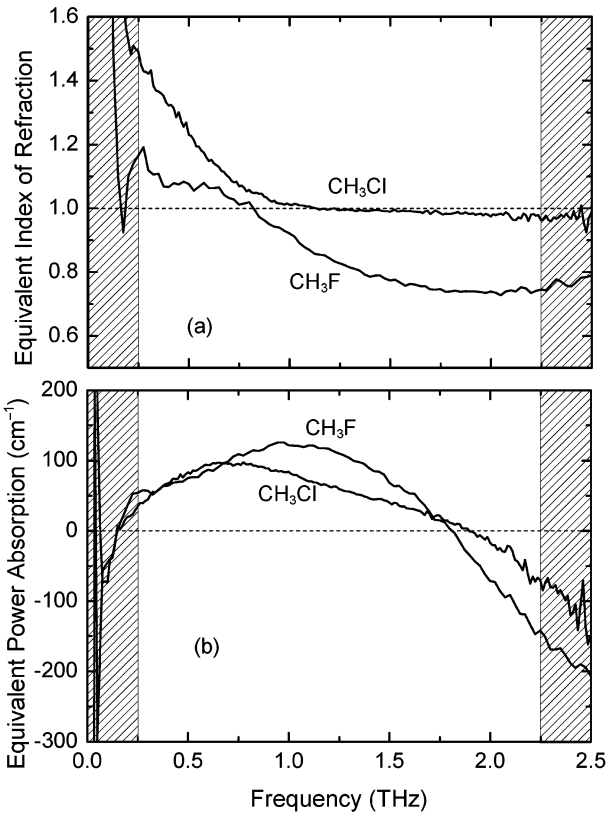

Figure 13. (a) Equivalent index of refraction and (b) equivalent power absorption coefficient of the adsorbed submonolayers of CH_3Cl and CH_3F.

tion-induced absorption is observed in the low-frequency range from 0.2 to 1.6 THz, while at higher frequencies, the adsorption of CH_3Cl causes a decrease in the absorption of the aerogel sample, resulting in a signal increase in the transmitted pulse.

Figure 12a presents the transmitted THz pulses in the aerogel sample in a vacuum and after the CH_3F adsorption, with the latter shifted for clarity. The equally spaced transients following the main pulse depict the uniformly spaced rotational absorption lines of CH_3F. In the enlargement of pulses in the vicinity of the main pulses shown in the inset, again no significant time delay is observed for the two pulses. The respective spectra of the main transmitted pulses in the time range of 0−20 ps are presented in Figure 12b; the corresponding spectrum ratio is shown in Figure 12c. Here, the adsorption-induced absorption is in the range from 0.2 to 2.0 THz, while above 2.0 THz, the passivated −OH groups by the adsorbed CH_3F molecules cause the absorption decrease in the sample scan.

With the above results, we can now calculate the equivalent index of refraction and equivalent power absorption coefficient for the adsorbed CH_3Cl and CH_3F. For this purpose, the equivalent bulk layer thicknesses are calculated and listed in Table 1 as $d_E = 20.1$ μm for CH_3Cl and $d_E = 11.1$ μm for CH_3F. The calculated equivalent indices of refraction and equivalent power absorption coefficients for both the adsorbed CH_3Cl and CH_3F are shown in parts a and b, respectively, of Figure 13. Since the index of refraction and power absorption coefficient for the bulk materials are not available, a corresponding comparison is not given here. As mentioned earlier, compared with the adsorptions of water and ammonia, the adsorptions of CH_3Cl and CH_3F are roughly 1 order of magnitude weaker in the hydrophilic silica aerogel. However, the absorption properties are very similar. At low frequencies, the adsorptions cause an increase in the absorption of the aerogel sample, but at higher frequencies, the absorption decrease caused by the passivated −OH groups dominates the absorption increase due to the adsorbed molecules, resulting in a net decrease in the power absorption. It is interesting to note that, as shown in Figure 13a, above a certain frequency, the equivalent index of refraction is below 1 for both the adsorbed CH_3Cl and CH_3F. This is consistent with the fact that no time delay is observed between the pulses in a vacuum and the pulses after CH_3Cl and CH_3F adsorption. These results show that the adsorbed CH_3Cl and CH_3F molecules greatly modified the dielectric properties of the hydrophilic silica aerogel, which might be useful in tailoring the properties of the silica aerogels.

6. Adsorption with Other Gases. THz-TDS was also used to study the adsorption of hydrogen (H_2) and carbon monoxide (CO) in hydrophilic silica aerogel. For H_2 adsorption, the sample chamber was filled with H_2 and kept at 20 Torr for over 10 h. Before and during this process, sample and reference scans were taken to monitor the property changes in aerogel. However, our THz-TDS results showed no noticeable change. A similar experiment was conducted for dosing with CO; again we did not observe any noticeable effect.

THz-TDS is very effective in obtaining dielectric properties of materials in the broad frequency range of 0.1−5 THz. In monitoring the property changes of the material, this method is limited by the stability of the laser system used, and environmental factors such as room temperature fluctuations. Therefore, this method may not be able to tell the small changes in material properties such as a minimal amount of adsorption in aerogel.

However, the volumetric method is more accurate in that it directly monitors the pressure change due to adsorption; therefore, it is only limited by the accuracy of the pressure gauge and the airtightness of the vacuum system. Our vacuum system has been previously leak-checked and is believed to have a leak rate of less than 0.01 Torr/h. With this we believe that the volumetric method is more sensitive than THz-TDS in monitoring adsorption change.

To examine the adsorption of H_2 and CO with aerogel, a separate experiment was conducted using solely the volumetric method. In this experiment, we repeated the volume-measuring experiment by filling the dosing chamber with 99.68 Torr of nitrogen gas, which is very close to the pressures we will use for filling with H_2 and CO, to minimize the calculation error in obtaining the initial pressure. The sample chamber containing the hydrophilic silica aerogel was then opened to the dosing chamber. An equilibrium pressure of 75.87 Torr was reached after a few minutes. We assume that there is no adsorption of nitrogen in aerogel, so the two pressures follow the ideal gas law. After the system was pumped down below 50 mTorr, the dosing chamber was filled with 99.29 Torr of H_2. When the sample chamber was opened to the dosing chamber, the equilibrium pressure was 75.57 Torr after a few minutes. This pressure is equal to that calculated from the ideal gas law with the dosing and equilibrium pressures of nitrogen, indicating that there was no adsorption of H_2 in the first few minutes of dosing. This pressure was maintained for over 1 h, during which the pressure gauge reading remained constant, showing no observed adsorption. A similar experiment was conducted for CO, and again no adsorption was observed.

IV. Conclusion

The THz-TDS technique has been used to study silica aerogels. Our measurements show that dry hydrophilic and hydrophobic silica aerogels have similar but discernible refractive indices in the THz range, but starting from ~1 THz, the absorption of the hydrophilic sample increases more rapidly with frequency than that of the hydrophobic sample. Adsorption study of H_2O and D_2O vapor in a hydrophilic sample shows that the Si−OH groups are responsible for the absorption increase of the dry hydrophilic sample for frequencies above 1 THz. The THz absorption of the hydrophilic sample with the adsorbed molecules H_2O, D_2O, NH_3, CH_3Cl, and CH_3F is determined by two effects: first an increase in absorption due to the adsorbed molecules themselves and second a decrease in absorption as a result of the adsorbed molecules passivating the Si−OH groups. The two competing effects result in a decrease in absorption for frequencies above 1 THz with a low dosing amount. For the adsorption of water, as the dosing pressure increases, the overall absorption increases in the entire frequency range from 0.2 to 3.0 THz, which is consistent with the previous report that the adsorbed water molecules build up clusters around the surface hydroxyl groups. In the dosing pressure range in our experiment, the spectrum amplitude of the sample with adsorbed water is always higher than that of the original sample at the high-frequency end.

The surface −OH groups in hydrophilic silica aerogel can be replaced by −OD groups by dosing with D_2O vapor, causing an observable change in the index of refraction and absorption. This replacement is fully reversible by dosing with H_2O. The adsorbed water, ammonia, methyl chloride, and methyl fluoride are in submonolayer form; the adsorbed water and ammonia show dielectric properties different from those of the corresponding bulk materials. Both THz-TDS and the volumetric method are used for the study of dosing with H_2 and CO. However, no adsorption is observed for these two gases.

Acknowledgment. We thank Darpan Pradhan and Benjamin Lee for their invaluable work in constructing the mechanical balance. This work was partially supported by the National Science Foundation, the U.S. Army Research Office, and the Department of Energy.

References and Notes

(1) Kistler, S. S. Coherent expanded aerogels. *J. Phys. Chem.* **1932**, *36*, 52.

(2) Nappi, E. Aerogel and its applications to RICH detectors. *Nucl. Phys. B, Proc. Suppl.* **1998**, *61B*, 270.

(3) Rettelbach, Th.; Säuberlich, J.; Korder, S.; Fricke, J. Thermal conductivity of IR-opacified silica aerogel powders between 10 K and 275 K. *J. Phys. D* **1995**, *28*, 581.

(4) Reim, M.; Beck, A.; Körner, W.; Petricevic, R.; Glora, M.; Weth, M.; Schliermann, T.; Fricke, J.; Schmidt, Ch.; Pötter, F. J. Highly insulating aerogel glazing for solar energy usage. *Sol. Energy* **2002**, *72*, 21.

(5) Tsou, P. Silica aerogel captures cosmic dust intact. *J. Non-Cryst. Solids* **1995**, *186*, 415.

(6) Hair, M. L. *Infrared Spectroscopy in Surface Chemistry*; Marcel Dekker: New York, 1967.

(7) Peri, J. B. Infrared study of OH and NH_2 groups on the surface of a dry silica aerogel. *J. Phys. Chem.* **1966**, *70*, 2937.

(8) Grischkowsky, D.; Keiding, S.; van Exter, M.; Fattinger, Ch. Far-infrared time-domain spectroscopy with terahertz beams of dielectrics and semiconductors. *J. Opt. Soc. Am. B* **1990**, *7*, 2006.

(9) Wagh, P. B.; Ingale, S. V. Comparison of some physico-chemical properties of hydrophilic and hydrophobic silica aerogels. *Ceram. Int.* **2002**, *28*, 43.

(10) Zhang, J.; Grischkowsky, D. Terahertz time-domain spectroscopy of submonolayer water adsorption in hydrophilic silica aerogel. *Opt. Lett.* **2004**, *29*, 1031.

(11) Franks, F., Ed. *Water: A Comprehensive Treatise, Vol. 5: Water in Disperse Systems*; Plenum: New York, 1975.

(12) http://www.mkt-intl.com/aerogels/silica.html.

(13) Washburn, E. W., Ed. *International Critical Tables of Numerical Data, Physics, Chemistry and Technology*, 1st electronic ed.; Knovel: Norwich, NY, 2003; http://www.knovel.com/knovel2/Toc.jsp?SpaceID=10093&BookID=735.

(14) Schwertfeger, F.; Glaubitt, W.; Schubert, U. Hydrophobic aerogels from $Si(OMe)_4$/$MeSi(OMe)_3$ mixtures. *J. Non-Cryst. Solids* **1992**, *145*, 85.

(15) Young, G. J. Interaction of water vapor with silica surfaces. *J. Colloid Sci.* **1958**, *13*, 67.

(16) Pierre, A. C.; Pajonk, G. M. Chemistry of aerogels and their applications. *Chem. Rev.* **2002**, *102*, 4243.

(17) Wang, P.; Beck, A.; Körner, W.; Scheller, H.; Fricke, J. Density and refractive index of silica aerogels after low- and high-temperature supercritical drying and thermal treatment. *J. Phys. D.* **1994**, *27*, 414.

(18) Buzykaev, A. R.; Danilyuk, A. F.; Ganzhur, S. F.; Kravchenko, E. A.; Onuchin, A. P. Measurement of optical parameters of aerogel. *Nucl. Instrum. Methods, A* **1999**, *433*, 396.

(19) van Roosmalen, A. J.; Moi, J. C. An infrared study of the silica gel surface. 1. Dry silica gel. *J. Phys. Chem.* **1978**, *82*, 2748.

(20) Benesi, H. A.; Jones, A. C. An infrared study of the water-silica gel system. *J. Phys. Chem.* **1959**, *63*, 179.

(21) Zhang, J.; Grischkowsky, D. Waveguide terahertz time-domain spectroscopy of nanometer water layers. *Opt. Lett.* **2004**, *29*, 1617.

(22) Kindt, J. T.; Schmuttenmaer, C. A. Far-infrared dielectric properties of polar liquids probed by femtosecond terahertz pulse spectroscopy. *J. Phys. Chem.* **1996**, *100*, 10373.

(23) Harde, H.; Zhao, J.; Wolff, M.; Cheville, R. A.; Grischkowsky, D. THz time-domain spectroscopy on ammonia. *J. Phys. Chem. A* **2001**, *105*, 6038.

(24) Harde, H.; Katzenellenbogen, N.; Grischkowsky, D. Terahertz coherent transients from methyl chloride vapor. *J. Opt. Soc. Am. B* **1994**, *11*, 1018.

(25) Harde, H.; Cheville, R. A.; Grischkowsky, D. Terahertz studies of collision-broadened rotational lines. *J. Phys. Chem. A* **1997**, *101*, 3646.

(26) Harde, H.; Keiding, S.; Grischkowsky, D. Terahertz commensurate echoes: periodic rephrasing of molecular transients in free-induction decay. *Phys. Rev. Lett.* **1991**, *66*, 1834.